Zeolitic Imidazolate Frameworks as H_2 Adsorbents: Ab-Initio Based Grand Canonical Monte-Carlo Simulation

Sang Soo Han,*,† Seung-Hoon Choi,‡ and William A. Goddard III§

† *Center for Nanocharacterization, Korea Research Institute of Standards and Science, 209 Gajeong-ro, Yuseong-gu, Daejeon 305-340, Republic of Korea*

‡ *Insilicotech Co. Ltd., A-1101 Kolontripolis, 210, Geumgok-Dong, Bundang-Gu, Seongnam, Gyeonggi-Do 463-943, Republic of Korea*

§ *Materials and Process Simulation Center (MC 139-74), California Institute of Technology, Pasadena, California 91125*

* To whom correspondence should be addressed.
E-mail: sangsoo@kriss.re.kr

Supporting Information

S.1 Quantum mechanical calculations

In this work, we used a grand canonical Monte-Carlo (GCMC) simulation to simulate H_2 adsorption isotherms of zeolitic imidazolate frameworks (ZIFs). The accuracy of the GCMC simulation depends on accuracy of force fields (FFs). Thus we developed the FFs from high-level quantum mechanical (QM) calculations that provide a proper description of the London dispersion forces responsible for van der Waals attraction.

DFT methods are well-known to provide a poor description of van der Waals attraction, making it is unsuitable for predicting accurate interaction energies between H_2 and ZIFs. Therefore we used the second-order Møller-Passet (MP2) with the approximate resolution of the identity (RI-MP2).[S1,S2] These calculations were carried out with the Q-CHEM[S3] and TURBOMOLE[S4] programs.

For H_2---$C_3N_3H_3$, H_2---$C_3N_3(NO_2)_3$, and H_2---$C_3N_3Cl_3$, we used the aug-cc-pVQZ basis sets using the Q-CHEM program, and for H_2---ZnN_4H_8 we used the quadruple zeta valence basis (QZV) supplemented with polarization functions from the cc-pVTZ basis, which is denoted as QZVPP using the TURBOMOLE program. For each MP2 calculation, we considered two different H_2 configurations, and we did not include excitations out of the 1s core orbitals. In addition, the binding energies of H_2 were corrected for basis-set superposition error (BSSE) by the full counterpoise procedure.

In addition, we calculated H_2 binding energies to the six imidazolate linkers (IM, mIM, nIM, bIM, mbIM, and cbIM) by the RI-MP2 method. Here we first performed a geometry optimization process for each compound with the cc-pVDZ basis set, and then carried out a single

point energy calculation with the aug-cc-pVQZ basis set. Of course, the BSSE correction was also considered in this calculation. The calculated H_2 binding energies are summarized in Table S1.

Table S1. H_2 binding energies (kcal/mol) to the imidazole linkers and benzene derivatives calculated by the RI-MP2/aug-cc-pVQZ method.

	IM ($C_3N_2H_4$)	mIM ($C_4N_2H_6$)	nIM ($C_3N_3O_2H_3$)	bIM ($C_7N_2H_6$)	mbIM ($C_8N_2H_8$)	cbIM ($C_7N_2ClH_5$)	nbIM ($C_7N_3O_2H_5$)
H_2 binding energy	-1.256 (-1.118)[a]	-1.390 (-1.234)	-1.181 (-0.940)	-1.480 (-1.203)	-1.547 (-1.385)	-1.474 (-1.286)	-1.376 (-1.203)

	Benzene (C_6H_6)	Methylbenzene ($C_6H_5CH_3$)	Chlorobenzene (C_6H_5Cl)	Nitrobenzene ($C_6H_5NO_2$)
H_2 binding energy	-1.367 (-1.223)[a]	-1.490 (-1.333)	-1.343 (-1.185)	-1.233 (-1.089)

[a]BSSE corrected value

S.2 Fitting of the force field (FF)

We used MP2 calculations to determine interaction potential of H_2 with imidazolate organic linkers and Zn metallic joints of the ZIFs. Then we fitted these results to obtain Morse pair potentials (Eq. 1) between each atom of H_2 and ZIF.

$$U_{ij}(r_{ij}) = D\left\{\exp[\alpha(1-\frac{r_{ij}}{r_o})] - 2\cdot\exp[\frac{\alpha}{2}(1-\frac{r_{ij}}{r_o})]\right\} \quad (1)$$

Here the parameter D is the well depth, r_o is the equilibrium bond distance, and α determines the stiffness (force constant).

In the GCMC simulation for simulation of H_2 uptake in ZIFs, we need eight FFs to describe non-bonded interactions of H_2---H_2 and H_2---ZIFs such as H_A---H_A, H_A---C_R, H_A---C_3, H_A---H_, H_A---N_{IM}, H_A---N_{NO2}, H_A---O, H_A---Cl, and H_A---Zn, where H_A means a hydrogen atom in a H_2 molecule, C_R does an aromatic carbon atom, C_3 does a sp^3 carbon, and H_ does a hydrogen atom bonded to the aromatic carbon, N_{IM} does an nitrogen atom in an imdazolate linker, N_{NO2} does an nitrogen atom in a functional group ($-NO_2$), O does an oxygen atom in a functional group ($-NO_2$), Cl does a chlorine atom in a functional group ($-C_6H_5Cl$), and Zn does a zinc atom in a ZnN_4 metallic joint part. We previously developed FFs for H_2---MOF (metal-organic frameworks) and H_2---COF (covalent-organic framework), and then reproduced experimental H_2 isotherms of the MOFs and COFs with the developed FFs.[S5,S6] Thus of the eight FFs to simulate H_2 uptake in ZIFs, the first four FFs (H_A---H_A, H_A---C_R, H_A---C_3, and H_A---H_) could be used with ones developed in the previous works.[S5,S6]

For the H_A---N_{IM} FF, we carried out RI-MP2/aug-cc-pVQZ calculations for the interaction between H_2 and $C_3N_3H_3$ shown in Fig. S1(a). Here, for a parallel orientation of H_2, RI-MP2 calculation shows H_2 binding energy of -0.94 kcal/mol while our FF obtains -0.93 kcal/mol. For a vertical orientation of the H_2 the RI-MP2 leads to -0.77 kcal/mol while our FF leads to -0.78 kcal/mol.

For H_A---Cl FF, the comparison is shown in Fig. S1(b). Here, for a parallel orientation of H_2, RI-MP2 calculation obtains an H_2 binding energy of -1.43 kcal/mol while our FF leads to -1.36 kcal/mol. Also, for a vertical orientation of H_2 the RI-MP2 gets -0.78 kcal/mol while our FF leads to -1.10 kcal/mol.

For the H_A---N_{NO2} and H_A---O FF, the comparison of the RI-MP2/aug-cc-pVQZ calculation and our FF is shown in Fig. S1(c). Here, for a parallel orientation of H_2, RI-MP2 calculation shows an H_2 binding energy of -1.63 kcal/mol while our FF gets -1.61 kcal/mol. Also, for a vertical orientation of H_2 the RI-MP2 gets -0.71 kcal/mol while our FF gets -1.31 kcal/mol.

Moreover, for the H_A---Zn FF, we carried out RI-MP2/QZVPP calculations for the interaction between H_2 and ZnN_4H_8 shown in Fig. S1(d). Here, for a parallel orientation of H_2, RI-MP2 calculation finds an H_2 binding energy of -0.54 kcal/mol while our FF gets -0.56 kcal/mol. Also, for the vertical orientation of H_2 the RI-MP2 obtains -0.50 kcal/mol while our FF gets -0.49 kcal/mol. These results from our FF and from high level RI-MP2 calculations are summarized in Table S2.

Also, we need to mention that several ZIFs considered in this work have many disordered atoms in their crystal data obtained from the Cambridge Crystallographic Data Centre (CCDC). Handling of such disordered atoms could be critical for prediction of H_2 uptake of ZIFs with relatively small diameters because orientation of imidazolate linkers can drastically change the H_2-pore interaction. Therefore, we performed molecular mechanics to optimize their ZIF structures with unchanged lattice parameters before the GCMC simulation.

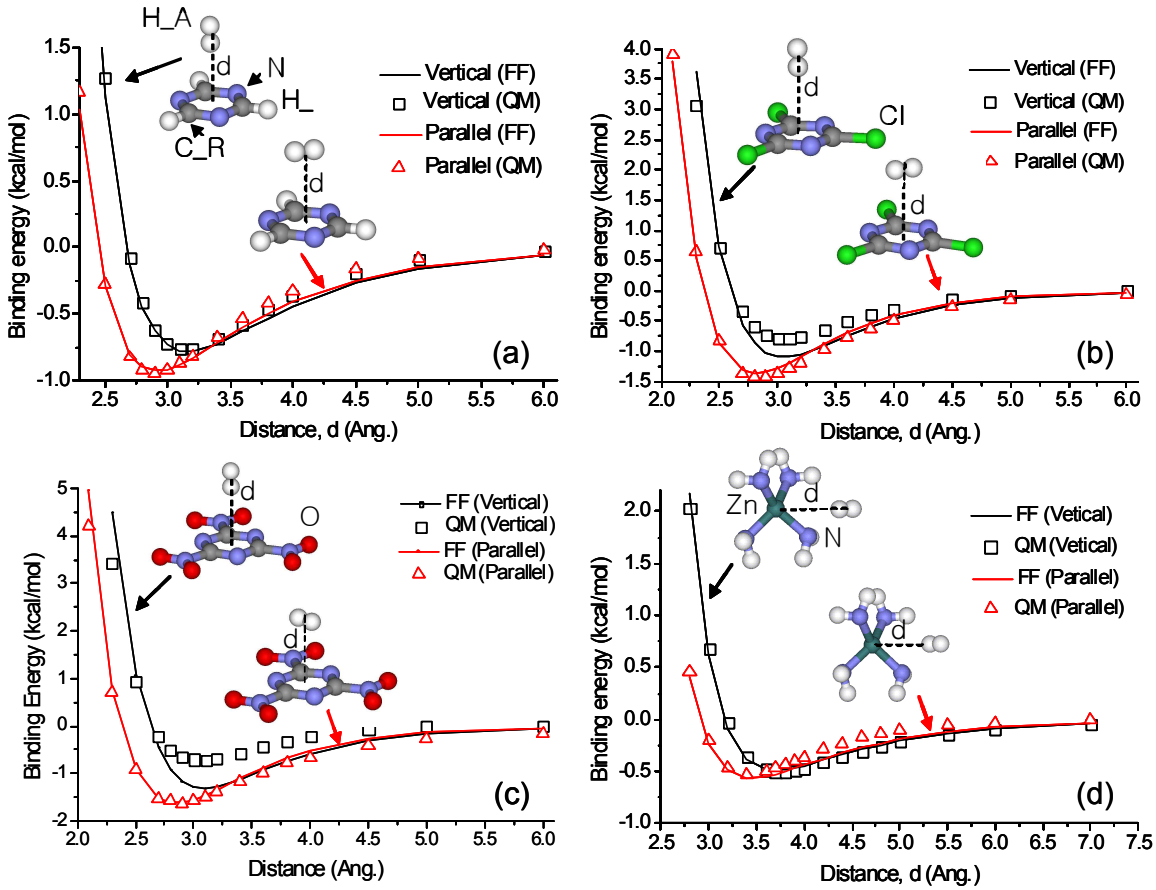

Figure S1. Comparison of the quantum calculations (RI-MP2) and fitted force fields for H_2 interacting with $C_3N_3H_3$ (a), $C_3N_3Cl_3$ (b), $C_3N_3(NO_2)_3$ (c), and ZnN_4H_8 (d). In these calculations, the H_2 was oriented parallel and vertical to the organic linker and metallic clusters where the distance between the bond midpoint of H_2 and the center of the organic linker and metallic clusters were varied.

Table S2. van der Waals FF parameters used in the GCMC simulations.

Term	D (kcal/mol)	r_0 (Å)	γ [a]
C_R---H_A	0.10082	3.12022	12.00625
H_---H_A	0.00087	3.24722	12.00625
H_A---H_A	0.01815	3.56980	10.70940
C_3---H_A	0.05239	3.02401	14.90625
N_{IM}---H_A	0.06300	3.30170	11.62254
N_{NO2}---H_A	0.07156	3.09389	10.29909
O_{NO2}---H_A	0.08482	3.63895	9.76998
Cl---H_A	0.15735	3.46095	13.90551
Zn---H_A	0.08067	3.53954	11.94487

[a] $\gamma=2r_0\alpha$. In the Cerius2 software, the γ is used as a default value in the FF file.

S.3 Simulated H_2 uptake capacities (77 and 300 K) of all ZIFs considered in this work

ZIF-2					
	77 K		300 K		Q_{st} (kJ/mol)
Pressure (bar)	Total (wt%)	Excess (wt%)	Total (wt%)	Excess (wt%)	
0.0001	0.004	0.004	-	-	6.183
0.01	0.130	0.130	-	-	6.201
0.1	1.048	1.047	0.004	0.004	6.287
0.2	1.657	1.656	0.008	0.007	6.329
0.3	2.069	2.066	0.011	0.010	6.353
0.4	2.324	2.321	0.014	0.012	6.363
0.5	2.556	2.552	0.017	0.015	6.375
0.6	2.711	2.706	0.019	0.017	6.378
0.7	2.826	2.820	0.021	0.018	6.387
0.8	2.951	2.944	0.023	0.020	6.384
0.9	3.044	3.038	0.025	0.021	6.392
1	3.107	3.100	0.027	0.0223	6.375
5	4.552	4.519	0.083	0.064	6.357
10	4.787	4.721	0.152	0.114	6.318
20	5.01	4.877	0.290	0.214	6.281
30	5.153	4.958	0.414	0.301	6.258
40	5.266	5.007	0.526	0.375	6.238
50	5.288	4.964	0.628	0.440	6.219
60	5.348	4.960	0.726	0.500	6.216
70	5.390	4.950	0.821	0.558	6.215
80	5.467	4.937	0.902	0.602	6.214
90	5.480	4.898	0.977	0.640	6.208
100	5.501	4.854	1.053	0.679	6.196

Here, Q_{st} is the isosteric heat of adsorption of H_2 from total uptake at 77 K

ZIF-3					
	77 K		300 K		Q_{st} (kJ/mol)
Pressure (bar)	Total (wt%)	Excess (wt%)	Total (wt%)	Excess (wt%)	
0.0001	0.016	0.016	-	-	8.464
0.01	0.441	0.441	-	-	8.374
0.1	1.321	1.320	0.005	0.004	7.723
0.2	1.726	1.724	0.009	0.008	7.477
0.3	2.050	2.047	0.013	0.012	7.249
0.4	2.236	2.231	0.017	0.015	7.241
0.5	2.391	2.386	0.020	0.018	7.162
0.6	2.521	2.514	0.024	0.020	7.093
0.7	2.699	2.691	0.027	0.023	7.076
0.8	2.783	2.774	0.029	0.025	7.022
0.9	2.884	2.874	0.032	0.027	6.998
1	2.954	2.943	0.034	0.029	6.973
5	4.718	4.665	0.101	0.075	6.604
10	5.079	4.975	0.168	0.118	6.476
20	5.412	5.206	0.305	0.203	6.372
30	5.598	5.288	0.432	0.280	6.327
40	5.667	5.255	0.550	0.348	6.284
50	5.778	5.263	0.659	0.407	6.255
60	5.841	5.223	0.757	0.455	6.259
70	5.903	5.182	0.854	0.501	6.228
80	5.959	5.135	0.937	0.535	6.228
90	5.990	5.063	1.019	0.567	6.194
100	6.015	4.985	1.098	0.597	6.194

Here, Q_{st} is the isosteric heat of adsorption of H_2 from total uptake at 77 K

ZIF-8					
	77 K		300 K		Q_{st} (kJ/mol)
Pressure (bar)	Total (wt%)	Excess (wt%)	Total (wt%)	Excess (wt%)	
0.01	0.041	0.041	-	-	5.311
0.1	0.208	0.206	0.002	0.002	5.339
0.2	0.379	0.375	0.005	0.004	5.358
0.3	0.546	0.541	0.007	0.005	5.378
0.4	0.713	0.706	0.009	0.007	5.396
0.5	0.853	0.845	0.011	0.008	5.409
0.6	0.969	0.960	0.013	0.010	5.421
0.7	1.091	1.080	0.015	0.011	5.425
0.8	1.187	1.175	0.017	0.013	5.432
0.9	1.270	1.257	0.019	0.014	5.440
1	1.352	1.337	0.020	0.015	5.435
5	2.830	2.761	0.066	0.039	5.424
10	3.117	2.980	0.104	0.050	5.337
20	3.428	3.156	0.170	0.061	5.217
30	3.620	3.212	0.236	0.073	5.141
40	3.757	3.214	0.301	0.084	5.084
50	3.879	3.202	0.362	0.091	5.053
60	3.930	3.117	0.425	0.100	5.015
70	4.007	3.059	0.483	0.105	4.995
80	4.067	2.984	0.537	0.104	4.969
90	4.091	2.871	0.594	0.108	4.950
100	4.129	2.773	0.644	0.104	4.933

Here, Q_{st} is the isosteric heat of adsorption of H_2 from total uptake at 77 K

ZIF-10					
	77 K		300 K		Q_{st} (kJ/mol)
Pressure (bar)	Total (wt%)	Excess (wt%)	Total (wt%)	Excess (wt%)	
0.0001	0.008	0.008	-	-	7.861
0.01	0.278	0.278	-	-	7.842
0.1	1.174	0.278	0.005	0.004	7.397
0.2	1.597	1.172	0.009	0.007	7.194
0.3	1.878	1.593	0.012	0.009	7.080
0.4	2.047	1.872	0.015	0.011	6.975
0.5	2.249	2.039	0.017	0.013	6.927
0.6	2.352	2.239	0.020	0.015	6.852
0.7	2.486	2.340	0.022	0.016	6.820
0.8	2.576	2.472	0.024	0.017	6.771
0.9	2.671	2.560	0.026	0.018	6.753
1	2.736	2.653	0.028	0.019	6.710
5	4.560	4.474	0.089	0.047	6.211
10	5.067	4.898	0.165	0.082	5.959
20	5.611	5.277	0.319	0.154	5.758
30	5.913	5.415	0.457	0.210	5.639
40	6.122	5.461	0.590	0.261	5.557
50	6.311	5.486	0.711	0.301	5.502
60	6.380	5.390	0.822	0.331	5.481
70	6.484	5.330	0.935	0.363	5.453
80	6.580	5.262	1.041	0.388	5.419
90	6.668	5.185	1.132	0.398	5.381
100	6.721	5.073	1.223	0.408	5.384

Here, Q_{st} is the isosteric heat of adsorption of H_2 from total uptake at 77 K

ZIF-11					
	77 K		300 K		Q_{st} (kJ/mol)
Pressure (bar)	Total (wt%)	Excess (wt%)	Total (wt%)	Excess (wt%)	
0.00001	0.174	0.174	-	-	14.627
0.01	1.103	1.103	-	-	11.078
0.1	1.776	1.774	0.004	0.003	10.093
0.2	1.967	1.964	0.007	0.006	9.864
0.3	2.087	2.083	0.009	0.007	9.728
0.4	2.166	2.160	0.011	0.009	9.651
0.5	2.221	2.215	0.012	0.010	9.584
0.6	2.275	2.267	0.014	0.011	9.522
0.7	2.313	2.304	0.015	0.012	9.485
0.8	2.346	2.335	0.017	0.013	9.438
0.9	2.356	2.344	0.018	0.014	9.427
1	2.393	2.380	0.019	0.015	9.378
5	2.910	2.845	0.073	0.053	8.729
10	3.130	2.999	0.138	0.100	8.340
20	3.401	3.140	0.261	0.184	7.976
30	3.568	3.177	0.372	0.256	7.769
40	3.641	3.120	0.464	0.310	7.627
50	3.725	3.074	0.560	0.368	7.542
60	3.784	3.003	0.642	0.412	7.474
70	3.863	2.951	0.725	0.457	7.451
80	3.892	2.849	0.792	0.486	7.387
90	3.922	2.749	0.852	0.508	7.352
100	3.958	2.654	0.909	0.528	7.331

Here, Q_{st} is the isosteric heat of adsorption of H_2 from total uptake at 77 K

ZIF-68					
	77 K		300 K		Q_{st} (kJ/mol)
Pressure (bar)	Total (wt%)	Excess (wt%)	Total (wt%)	Excess (wt%)	
0.0001	0.080	0.080	-	-	10.666
0.01	0.635	0.635	-	-	9.757
0.1	1.460	1.459	0.003	0.003	8.955
0.2	1.774	1.772	0.005	0.005	8.718
0.3	1.879	1.876	0.008	0.007	8.556
0.4	2.008	2.005	0.010	0.008	8.489
0.5	2.099	2.095	0.012	0.010	8.412
0.6	2.176	2.170	0.013	0.011	8.355
0.7	2.196	2.190	0.015	0.012	8.319
0.8	2.257	2.251	0.016	0.013	8.284
0.9	2.333	2.326	0.018	0.014	8.269
1	2.353	2.344	0.019	0.015	8.216
5	2.935	2.893	0.056	0.038	7.718
10	3.225	3.142	0.099	0.063	7.466
20	3.510	3.345	0.185	0.114	7.240
30	3.677	3.430	0.264	0.157	7.128
40	3.772	3.442	0.337	0.194	7.034
50	3.848	3.436	0.407	0.229	6.999
60	3.955	3.462	0.472	0.258	6.926
70	3.965	3.388	0.527	0.278	6.908
80	4.010	3.352	0.587	0.303	6.872
90	4.043	3.302	0.642	0.322	6.872
100	4.053	3.229	0.691	0.336	6.834

Here, Q_{st} is the isosteric heat of adsorption of H_2 from total uptake at 77 K

ZIF-69					
	77 K		300 K		Q_{st} (kJ/mol)
Pressure (bar)	Total (wt%)	Excess (wt%)	Total (wt%)	Excess (wt%)	
0.0001	0.101	0.101	-	-	11.450
0.01	0.806	0.805	-	-	10.384
0.1	1.404	1.404	0.003	0.002	9.525
0.2	1.605	1.604	0.005	0.004	9.286
0.3	1.707	1.706	0.007	0.006	9.117
0.4	1.819	1.817	0.009	0.008	9.020
0.5	1.882	1.880	0.010	0.009	8.924
0.6	1.937	1.934	0.012	0.011	8.888
0.7	1.984	1.982	0.013	0.012	8.821
0.8	2.032	2.029	0.015	0.013	8.775
0.9	2.067	2.064	0.016	0.014	8.716
1	2.093	2.089	0.017	0.015	8.659
5	2.676	2.657	0.050	0.040	8.125
10	2.885	2.849	0.089	0.070	7.945
20	3.081	3.009	0.162	0.125	7.790
30	3.213	3.105	0.231	0.175	7.706
40	3.294	3.150	0.296	0.222	7.655
50	3.317	3.138	0.356	0.263	7.616
60	3.395	3.180	0.409	0.297	7.614
70	3.422	3.172	0.459	0.329	7.572
80	3.438	3.152	0.503	0.355	7.530
90	3.463	3.140	0.546	0.380	7.516
100	3.492	3.134	0.581	0.397	7.495

Here, Q_{st} is the isosteric heat of adsorption of H_2 from total uptake at 77 K

ZIF-70					
	77 K		300 K		Q_{st} (kJ/mol)
Pressure (bar)	Total (wt%)	Excess (wt%)	Total (wt%)	Excess (wt%)	
0.0001	0.011	0.011	-	-	8.233
0.01	0.196	0.196	-	-	7.812
0.1	0.707	0.707	0.003	0.002	7.218
0.2	0.932	0.931	0.005	0.004	7.017
0.3	1.070	1.069	0.008	0.006	6.881
0.4	1.177	1.175	0.010	0.007	6.772
0.5	1.250	1.246	0.012	0.009	6.702
0.6	1.333	1.328	0.014	0.010	6.614
0.7	1.395	1.388	0.015	0.011	6.551
0.8	1.454	1.446	0.017	0.012	6.503
0.9	1.510	1.500	0.018	0.012	6.451
1	1.559	1.548	0.020	0.013	6.415
5	2.421	2.349	0.058	0.025	5.807
10	2.808	2.657	0.101	0.035	5.612
20	3.200	2.890	0.193	0.061	5.416
30	3.443	2.975	0.273	0.076	5.321
40	3.582	2.955	0.352	0.089	5.236
50	3.721	2.936	0.425	0.096	5.205
60	3.804	2.860	0.493	0.110	5.156
70	3.917	2.814	0.560	0.122	5.137
80	3.985	2.722	0.621	0.133	5.104
90	4.082	2.660	0.681	0.144	5.082
100	4.108	2.525	0.735	0.157	5.060

Here, Q_{st} is the isosteric heat of adsorption of H_2 from total uptake at 77 K

ZIF-78					
	77 K		300 K		Q_{st} (kJ/mol)
Pressure (bar)	Total (wt%)	Excess (wt%)	Total (wt%)	Excess (wt%)	
0.0001	0.184	0.184	-	-	11.849
0.01	1.103	1.103	-	-	10.500
0.1	1.591	1.591	0.003	0.003	9.962
0.2	1.769	1.768	0.006	0.006	9.700
0.3	1.850	1.849	0.008	0.008	9.552
0.4	1.928	1.927	0.010	0.010	9.445
0.5	2.010	2.010	0.012	0.012	9.321
0.6	2.058	2.057	0.014	0.013	9.265
0.7	2.107	2.106	0.015	0.015	9.225
0.8	2.133	2.131	0.017	0.016	9.159
0.9	2.177	2.175	0.018	0.017	9.123
1	2.194	2.193	0.020	0.018	9.077
5	2.639	2.630	0.059	0.053	8.598
10	2.820	2.802	0.107	0.094	8.435
20	2.977	2.942	0.198	0.173	8.312
30	3.063	3.010	0.278	0.240	8.231
40	3.127	3.057	0.351	0.301	8.183
50	3.133	3.045	0.410	0.347	8.159
60	3.151	3.045	0.474	0.399	8.150
70	3.197	3.073	0.526	0.438	8.144
80	3.222	3.081	0.575	0.474	8.107
90	3.255	3.096	0.621	0.508	8.048
100	3.259	3.083	0.665	0.540	8.042

Here, Q_{st} is the isosteric heat of adsorption of H_2 from total uptake at 77 K

ZIF-79					
	77 K		300 K		Q_{st} (kJ/mol)
Pressure (bar)	Total (wt%)	Excess (wt%)	Total (wt%)	Excess (wt%)	
0.0001	0.009	0.009	-	-	11.286
0.01	0.685	0.685	-	-	9.785
0.1	1.229	1.228	0.002	0.002	9.054
0.2	1.456	1.455	0.004	0.004	8.855
0.3	1.557	1.555	0.006	0.005	8.757
0.4	1.626	1.623	0.008	0.007	8.640
0.5	1.682	1.679	0.010	0.008	8.607
0.6	1.762	1.758	0.011	0.009	8.508
0.7	1.791	1.786	0.012	0.010	8.477
0.8	1.829	1.823	0.014	0.011	8.440
0.9	1.873	1.867	0.015	0.012	8.384
1	1.890	1.883	0.016	0.013	8.333
5	2.467	2.434	0.047	0.033	7.732
10	2.756	2.690	0.081	0.052	7.439
20	3.054	2.923	0.151	0.093	7.176
30	3.183	2.986	0.215	0.128	7.049
40	3.296	3.034	0.275	0.159	6.975
50	3.397	3.070	0.330	0.186	6.873
60	3.494	3.102	0.384	0.211	6.827
70	3.509	3.051	0.431	0.229	6.804
80	3.586	3.063	0.476	0.246	6.769
90	3.591	3.002	0.523	0.264	6.758
100	3.594	2.940	0.570	0.282	6.716

Here, Q_{st} is the isosteric heat of adsorption of H_2 from total uptake at 77 K

S.4 Relationship between the isosteric heat of adsorption (Q_{st}) and pore size in five ZIFs of the GME topology

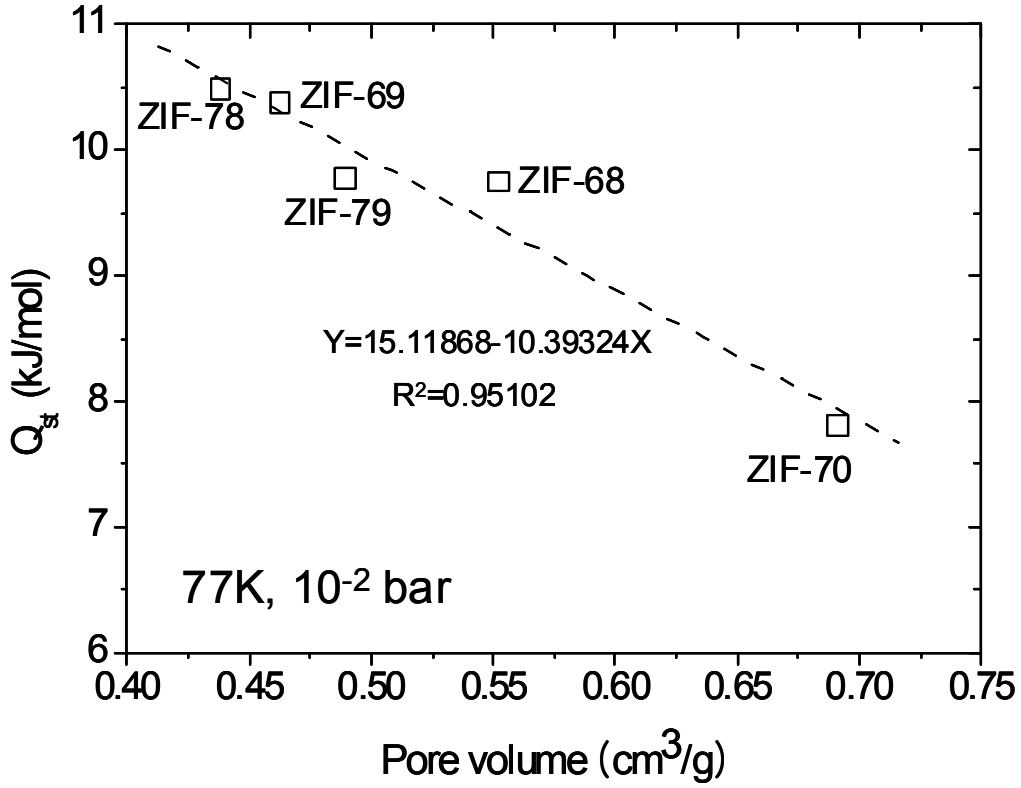

Figure S2. Relationship between Qst and pore size in five ZIFs of the GME topology. Here the Q_{st} value is inversely proportional to pore volume of ZIFs.

S.5 H_2 adsorption sites in all ZIFs considered in this work

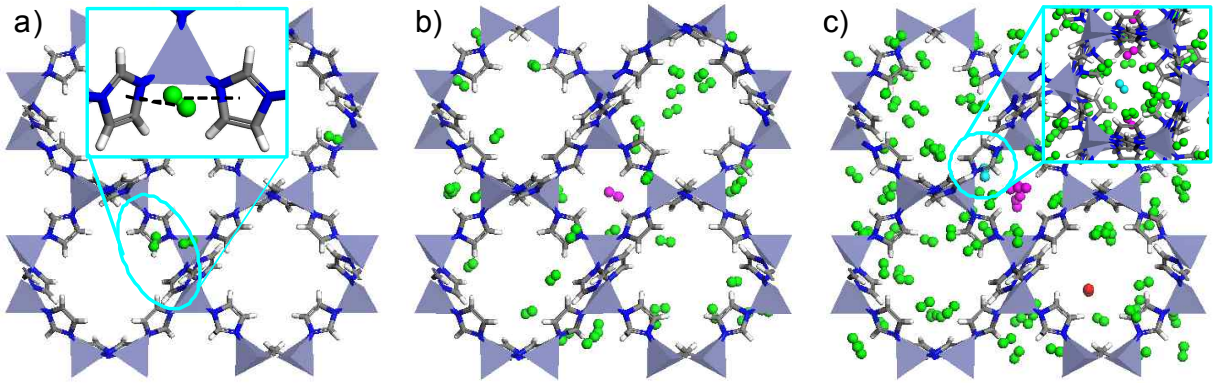

Figure S3. GCMC snapshots for ZIF-2 at 77 K with pressure, (a) 10^{-2} bar, (b) 10^{-1} bar, and (c) 1 bar. Here the preferential H_2 adsorption site (green) is on two IM linkers, the second site (pink) is the center of the four-ring opening channel, the third site (cyan) is the center of the six-ring opening channel, and the fourth site (red) is the center of the eight-ring opening channel.

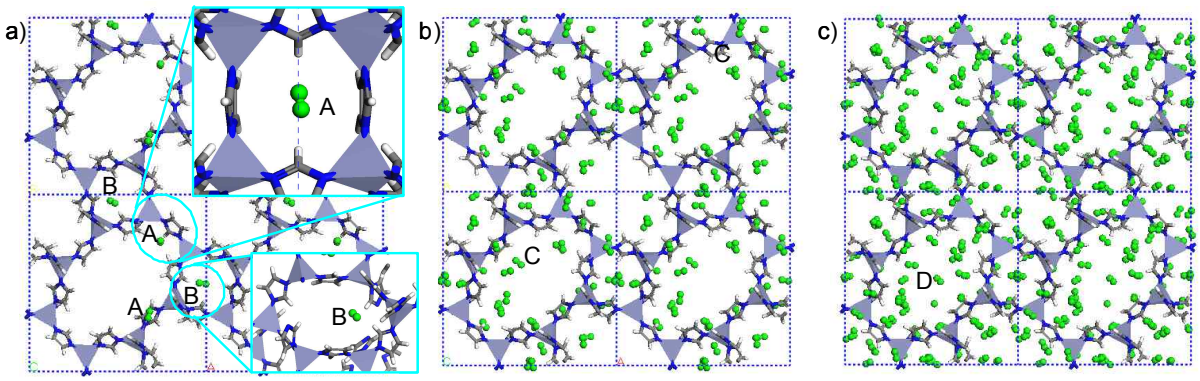

Figure S4. GCMC snapshots for ZIF-3 at 77 K with pressure, (a) 10^{-2} bar, (b) 10^{-1} bar, and (c) 10 bar. Here green molecules are H_2 adsorbed in ZIF-3. H_2 molecules (denoted as A) are preferentially adsorbed in the center of the four-ring opening channel in which they are sandwiched between two imidazolate linkers. The second preferential adsorption site (B) of H_2 is the center of the six-ring opening channel, and the third adsorption site (C) is on the IM linker in the eight-ring opening. In addition, the fourth site (D) is the center of the eight-ring opening channel.

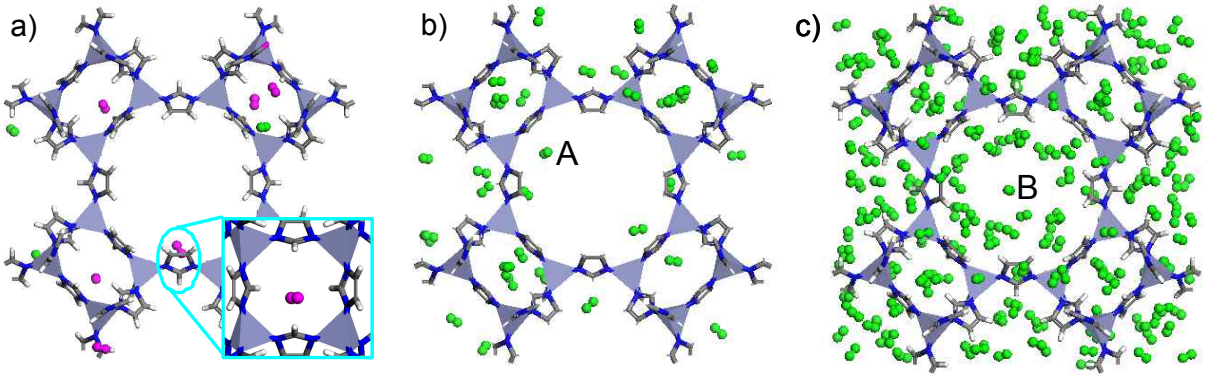

Figure S5. GCMC snapshots for ZIF-10 at 77 K with pressure, (a) 10^{-2} bar, (b) 10^{-1} bar, and (c) 10^{2} bar. The H_2 molecules (pink) are preferentially adsorbed in the center of the four-ring opening channel in which they are sandwiched between two IM linkers. Also, the second preferential adsorption site of H_2 (A) is on the five-membered ring of an imidazolate linker, and the third site (B) is the center of the eight-ring opening channel.

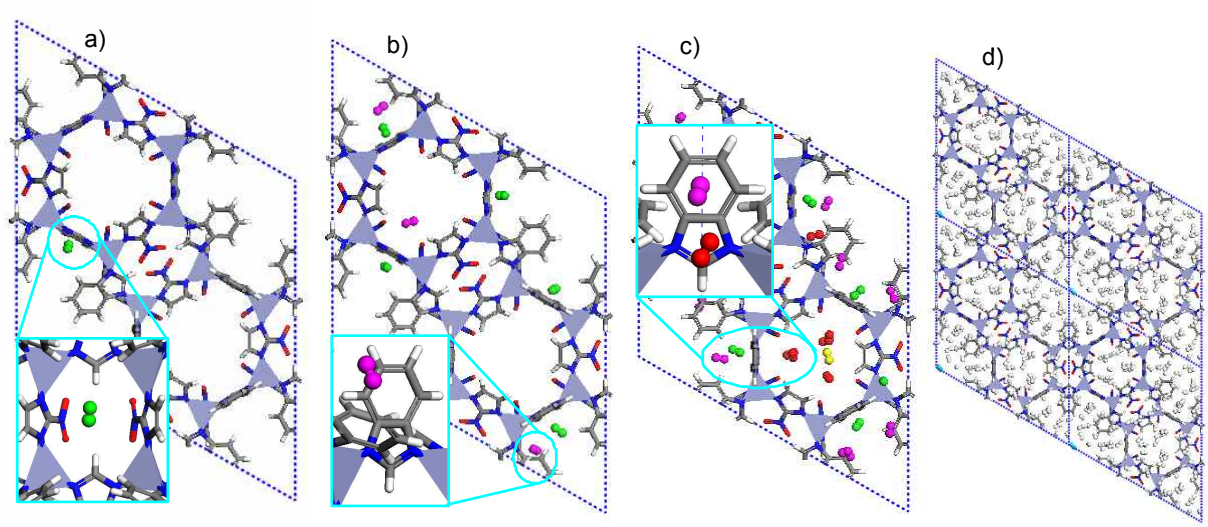

Figure S6. GCMC snapshots for ZIF-68 at 77 K with pressure, (a) 10^{-4} bar, (b) 10^{-3} bar, (c) 10^{-2} bar, and (d) 10^{2} bar. Here the first preferential adsorption site of H_2 (green) is the center of four-membered opening channel (sandwithed between four organic linkers) (Fig. a), the second site (pink) is on the six-membered ring of the bIM (Fig. b), the third site (red) is on the five-membered ring of the bIM (Fig. c), the fourth adsorption site (yellow) is the center of the six-membered opening channel (Fig. c), and the fifth site (cyan) is the center of the twelve-membered opening channel (Fig. d).

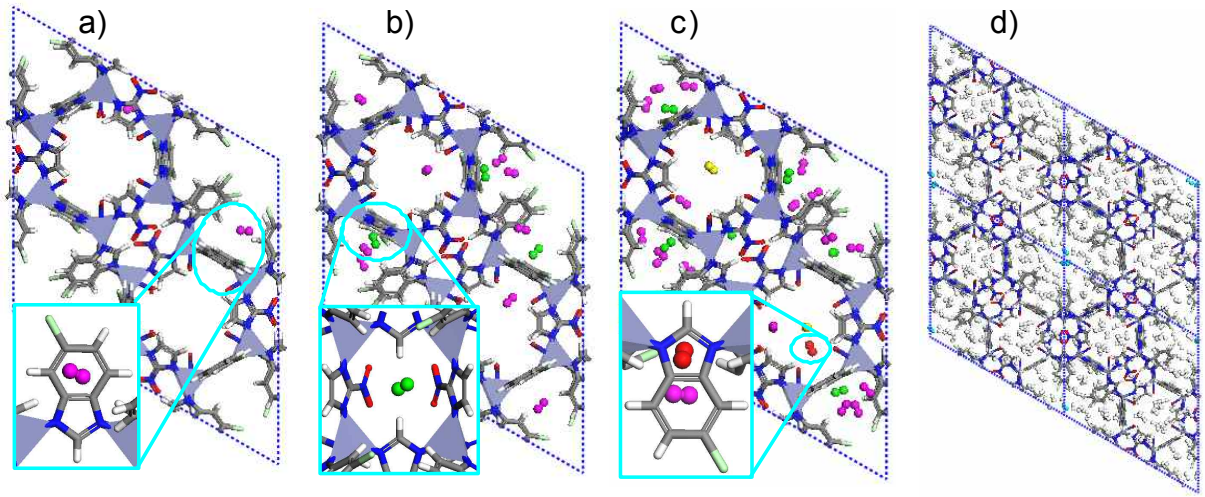

Figure S7. GCMC snapshots for ZIF-69 at 77 K with pressure, (a) 10^{-4} bar, (b) 10^{-3} bar, (c) 10^{-2} bar, and (d) 10^{2} bar. Here the first preferential adsorption site of H_2 (pink) is on the six-membered ring of the cbIM (Fig. a), the second site (green) is the center of four-membered opening channel (sandwithed between four organic linkers) (Fig. b), the third site (red) is on the five-membered ring of the cbIM (Fig. c), the fourth adsorption site (yellow) is the center of the six-membered opening channel (Fig. c), and the fifth site (cyan) is the center of the twelve-membered opening channel (Fig. d).

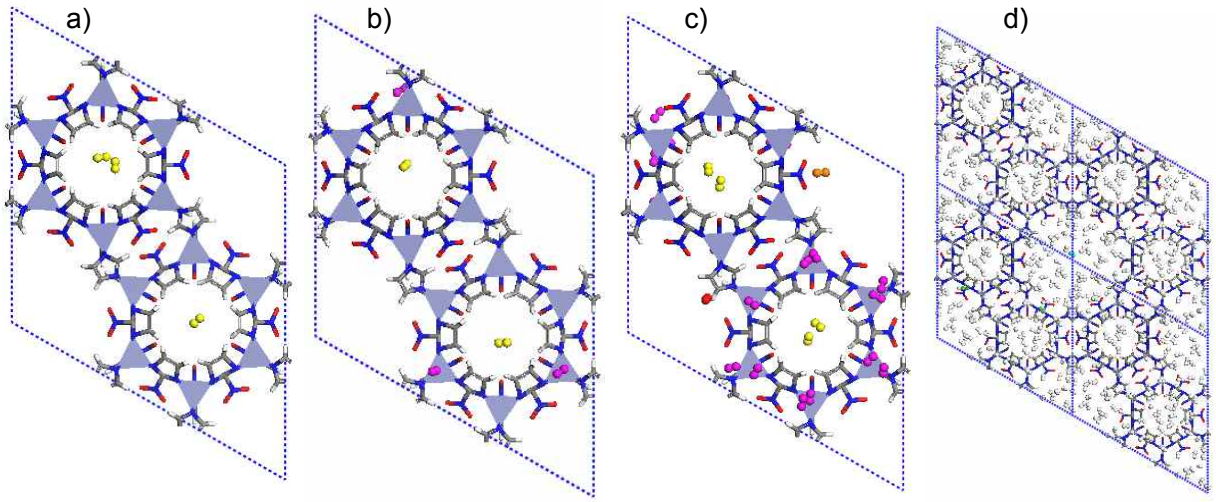

Figure S8. GCMC snapshots for ZIF-70 at 77 K with pressure, (a) 10^{-3} bar, (b) 10^{-2} bar, (c) 10^{-1} bar, and (d) 10^{2} bar. The first preferential adsorption site of H_2 (yellow) is the center of six-membered ring channel ring (Fig. a), the second site (pink) is nearby the ZnN_4 metallic nodes (Fig. b), the third site (red) is on the IM linker (Fig. c), the fourth site (orange) is on the nIM linker (Fig. c), and the fifth (green) and sixth (cyan) sites are the center of four-membered opening channel (sandwiched between four nIM linkers) (Fig. d) and the center of twelve-membered opening channel (Fig. d), respectively.

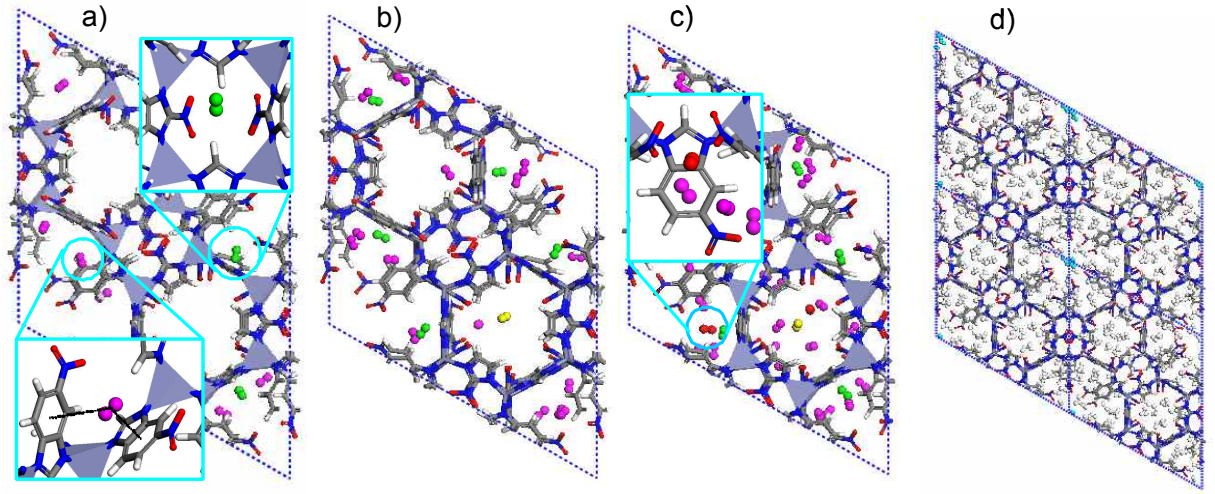

Figure S9. GCMC snapshots for ZIF-78 at 77 K with pressure, (a) 10^{-4} bar, (b) 10^{-3} bar, (c) 10^{-2} bar, and (d) 10^{2} bar. Here the first preferential adsorption site of H_2 (pink) is on the six-membered ring of the nbIM (Fig. a), the second site (green) is the center of four-membered opening channel (sandwithed between four organic linkers) (Fig. a), the third site (yellow) is the center of the six-membered opening channel (Fig. b), the fourth adsorption site (red) is on the five-membered ring of the nbIM (Fig. c), and the fifth site (cyan) is the center of the twelve-membered opening channel (Fig. d).

Table S3. H_2 Adsorption sites and their binding energy (kJ/mol) in all ZIFs considered in this work

ZIF	Component	H_2 adsorption site	H_2 binding energy
ZIF-2	ZnN_4, IM	(1) On the two IM linkers	-7.1
		(2) Center of the four-ring opening channel	-6.7
		(3) Center of the six-ring opening channel	-4.7
		(4) Center of the eight-ring opening channel	-3.3
ZIF-3	ZnN_4, IM	(1) Center of the four-ring opening channel	-9.2
		(2) Center of the six-ring opening channel	-8.4
		(3) On the IM linker	-5.9
		(4) Center of the eight-ring opening channel	-2.5
ZIF-8	ZnN_4, mIM	(1) On the mIM linker	-6.0
		(2) Center of the six-ring opening channel	-3.7
ZIF-10	ZnN_4, IM	(1) Center of the four-ring opening channel	-8.1
		(2) On the IM linker	-3.5
		(3) Center of the eight-ring opening channel	-2.7
ZIF-11	ZnN_4, bIM	(1) On the five-membered ring of the bIM linker	-14.9
		(2) Center of the four-ring opening channel	-11.1
		(3) Center of the six-ring opening channel	-9.5
		(4) Center of the eight-ring opening channel	-8.5
		(5) On the six-membered ring of the bIM linker	-7.5

Table S3. Continued

ZIF	Component	H_2 adsorption site	H_2 binding energy
ZIF-68	ZnN_4, nIM, bIM	(1) Center of the four-ring opening channel	-11.6
		(2) On the six-membered ring of the bIM linker	-9.5
		(3) On the five-membered ring of the bIM linker	-8.9
		(4) Center of the eight-ring opening channel	-7.9
		(5) Center of the twelve-ring opening channel	-1.4
ZIF-69	ZnN_4, nIM, cbIM	(1) On the six-membered ring of the cbIM linker	-12.3
		(2) Center of the four-ring opening channel	-11.1
		(3) On the five-membered ring of the cbIM linker	-8.8
		(4) Center of the eight-ring opening channel	-7.6
		(5) Center of the twelve-ring opening channel	-1.9
ZIF-70	ZnN_4, nIM, IM	(1) Center of the six-ring opening channel	-8.3
		(2) Nearby the ZnN_4 metallic node	-6.8
		(3) On the IM linker	-4.7
		(4) On the nIM linker	-4.0
		(5) Center of the twelve-ring opening channel	-1.4
		(6) Center of the four-ring opening channel	-0.6

Table S3. Continued

ZIF	Component	H_2 adsorption site	H_2 binding energy
ZIF-78	ZnN_4, nIM, nbIM	(1) On the six-membered ring of the nbIM linker	-12.7
		(2) Center of the four-ring opening channel	-11.6
		(3) Center of the eight-ring opening channel	-9.1
		(4) On the five-membered ring of the nbIM linker	-8.3
		(5) Center of the twelve-ring opening channel	-4.2
ZIF-79	ZnN_4, nIM, mbIM	(1) On the six-membered ring of the mbIM linker	-12.0
		(2) Center of the four-ring opening channel	-11.3
		(3) On the five-membered ring of the mbIM linker	-8.6
		(4) Center of the eight-ring opening channel	-7.9
		(5) Center of the twelve-ring opening channel	-1.6

S.6 References

S1. Weigend, F.; Häser, M. *Thero. Chem. Acc.* **1997**, *97*, 331.

S2. Ahlrichs, R.; Bar, M.; Häser, M.; Horn, H.; Kölmel, *Chem. Phys. Lett.* **1989**, *162*, 165.

S3. Q-CHEM software (Version 3.2, Q-Chem Inc., Pittsburgh)

S4. TURBOMOLE software (Version 5-7, University of Karlsruhe, Germany)

S5. Han, S. S.; Deng, W. Q.; Goddard, W. A. III *Angew. Chem. Int. Ed.* **2007**, *46*, 6289.

S6. Han, S. S.; Furukawa, H.; Yaghi, O. M.; Goddard, W. A. III *J. Am. Chem. Soc.* **2008**, *130*, 11580.